Manuscript prepared for Atmos. Chem. Phys. Discuss.
with version 2014/07/29 7.12 Copernicus papers of the LaTeX class copernicus.cls.
Date: 15 May 2015

Quantifying contributions to the recent temperature variability in the tropical tropopause layer

W. Wang[1,2], K. Matthes[2, 3], and T. Schmidt[4]

[1]Freie Universität Berlin, Institut für Meteorologie, Berlin, Germany
[2]GEOMAR Helmholtz-Zentrum für Ozeanforschung Kiel, Kiel, Germany
[3]Christian-Albrechts Universität zu Kiel, Kiel, Germany
[4]Helmholtz Zentrum Potsdam, Deutsches GeoForschungsZentrum (GFZ), Potsdam, Germany

Correspondence to: W. Wang (wuke.wang@fu-berlin.de)

Abstract

The recently observed variability in the tropical tropopause layer (TTL), which features a warming of 0.9 K over the past decade (2001–2011), is investigated with a number of sensitivity experiments from simulations with NCAR's CESM-WACCM chemistry-climate model. The experiments have been designed to specifically quantify the contributions from natural as well as anthropogenic factors, such as solar variability (Solar), sea surface temperatures (SSTs), the Quasi-Biennial Oscillation (QBO), stratospheric aerosols (Aerosol), greenhouse gases (GHGs), as well as the dependence on the vertical resolution in the model. The results show that, in the TTL from 2001 through 2011: a cooling in tropical SSTs leads to a weakening of tropical upwelling around the tropical tropopause and hence relative downwelling and adiabatic warming of 0.3 K decade^{-1}; stronger QBO westerlies result in a 0.2 K decade^{-1} warming; increasing aerosols in the lower stratosphere lead to a 0.2 K decade^{-1} warming; a prolonged solar minimum contributes about 0.2 K decade^{-1} to a cooling; and increased GHGs have no significant influence. Considering all the factors mentioned above, we compute a net 0.5 K decade^{-1} warming, which is less than the observed 0.9 K decade^{-1} warming over the past decade in the TTL. Two simulations with different vertical resolution show that, with higher vertical resolution, an extra 0.8 K decade^{-1} warming can be simulated through the last decade, compared with results from the "standard" low vertical resolution simulation. Model results indicate that the recent warming in the TTL is partly caused by stratospheric aerosols and mainly due to internal variability, i.e. the QBO and tropical SSTs. The vertical resolution can also strongly influence the TTL temperature response in addition to variability in the QBO and SSTs.

1 Introduction

The TTL is the transition layer from the upper troposphere to the lower stratosphere in the tropics, within which the air has distinct properties of both the troposphere and the stratosphere. The vertical range of the TTL depends on how it is defined, i.e., it can be a shallower

layer between 14–18.5 km (Fueglistaler et al., 2009) or a deeper layer of about 12–19 km (Gettelman and Forster, 2002; SPARC-CCMVal, 2010, chapter 7). As a key region for the stratosphere-troposphere coupling, the TTL acts like a "gate" for air entering into the stratosphere from the tropical troposphere. The temperature in the TTL is determined by the combined influences of latent heat release, thermally as well as dynamically driven vertical motion, and radiative cooling (Gettelman and Forster, 2002; Fueglistaler et al., 2009; Grise and Thompson, 2013). The thermal structure, static stability and zonal winds in the TTL affect the two-way interaction between the troposphere and the stratosphere (Flury et al., 2013; Simpson et al., 2009) as well as the surface climate, since the relative minimum temperature (usually known as the cold point tropopause, CPT) subsequently influences the radiation and water vapor budget (Andrews, 2010). The TTL reacts particularly sensitively to anthropogenically induced radiative, chemical and dynamical forcings of the climate system, and hence is a useful indicator for climate change (Fueglistaler et al., 2009).

Over the past decade, a remarkable warming has been captured by Global Positioning System Radio Occultation (GPS-RO) data in the TTL region (Schmidt et al., 2010; Wang et al., 2013). This might indicate a climate change signal, with possible important impacts on stratospheric climate, e.g., tropical tropopause temperatures dominate the amount of water vapor entering the stratosphere (Dessler et al., 2013, 2014; Solomon et al., 2010; Gettelman et al., 2009; Randel and Jensen, 2013). So far a long-term cooling in the lower stratosphere has been reported from the 1970s to 2000, although there are large differences between different data sets (Randel et al., 2009; Wang et al., 2012; Fueglistaler et al., 2013). The exact reason of the recent warming is therefore of great interest. An interesting question is also whether this warming will continue or change in sign in the future, and how well climate models can reproduce such a strong warming over one decade or longer time periods.

Based on model simulations, Wang et al. (2013) suggested that the warming around the tropical tropopause could be a result of a weaker tropical upwelling, which implies a weakening of the Brewer–Dobson circulation (BDC). However, the strengthening or weakening of

the BDC is still under debate (Butchart, 2014, and references therein). Results from observations indicate that the BDC may have slightly decelerated (Engel et al., 2009; Stiller et al., 2012), while estimates from a number of Chemistry-Climate Models (CCMs) show in contrast a strengthening of the BDC (Butchart et al., 2010; Li et al., 2008; Butchart, 2014). The reason for the discrepancy between observed and modeled BDC changes, as well as the mechanisms of the BDC response to climate change, are still under discussion (Oberländer et al., 2013; Shepherd and McLandress, 2011). The trends in the BDC may be different in different branches of the BDC (Lin and Fu, 2013; Oberländer et al., 2013). Bunzel and Schmidt (2013) show that the model configuration, i.e. the vertical resolution and the vertical extent of the model, can also impact trends in the BDC.

There are a number of other natural and anthropogenic factors besides the BDC, which influence radiative, chemical and dynamical processes in the TTL. One prominent candidate for natural variability is the sun, which provides the energy source of the climate system. The 11 year solar cycle is the most prominent natural variation on the decadal time scale (Gray et al., 2010). Solar variability influences the temperature through direct radiative effects and indirectly through radiative effects on ozone as well as indirect dynamical effects. The maximum response in temperature occurs in the equatorial upper stratosphere during solar maximum conditions, and a distinct secondary temperature maximum can be found in the equatorial lower stratosphere around 100 hPa (SPARC-CCMVal, 2010; Gray et al., 2010).

SSTs also influence the TTL by affecting the dynamical conditions and subsequently the propagation of atmospheric waves and hence the circulation. Increasing tropical SSTs can enhance the BDC, which in turn cools the tropical lower stratosphere through enhanced upwelling (Grise and Thompson, 2012, 2013; Oberländer et al., 2013). The QBO is the dominant mode of variability throughout the equatorial stratosphere, and has important impacts on the temperature structure as well as the distribution of chemical constituents like water vapor, methane and ozone (Baldwin et al., 2001). Beside the switch between easterlies and westerlies with a period of about 28 months, the QBO undergoes some cycle-to-cycle variability, e.g. variations in period, amplitude and shifts to westerlies or east-

erlies, which may influence the long-term variability in the TTL (Kawatani and Hamilton, 2013). Stratospheric aerosols absorb outgoing long-wave radiation and lead to additional heating in the lower stratosphere, which maximizes around 20 km (Solomon et al., 2011; SPARC-CCMVal, 2010, chapter 8).

While GHGs warm the troposphere, they cool the stratosphere at the same time by releasing more radiation into space. Warming of the troposphere and cooling of the stratosphere affect the temperature in the TTL directly, and also indirectly, by changing chemical trace gas distributions and wave activities (SPARC-CCMVal, 2010).

In climate models, a sufficient high vertical resolution is important in order for models to correctly represent dynamical processes, such as wave propagation into the stratosphere and wave-mean flow interactions. High-vertical resolution is also important to generate a self-consistent QBO (Richter et al., 2014). Meanwhile, vertical resolution is essential for a proper representation of the thermal structure in the model, e.g. models with coarse vertical resolution can not simulate the tropopause inversion layer (TIL, a narrow band of temperature inversion above the tropopause associated with a region of enhanced static stability) well (Wang et al., 2013; SPARC-CCMVal, 2010, chapter 7). Coarse vertical resolution is also still a problem for analysing the effects of El-Niño Southern Oscillation (ENSO) and the QBO onto the tropical tropopause (Zhou et al., 2001; SPARC-CCMVal, 2010, chapter 7).

In this study we use a series of simulations with NCAR's Community Earth System Model (CESM) model (Marsh et al., 2013), to quantify the contributions of the above discussed factors – Solar, SSTs, QBO, Aerosol and GHGs – to the recently observed variability in the TTL.

The details of the observational data, the model and numerical experiments, as well as a description of our methods are given in Sect. 2. The observed temperature variability in the TTL and the contributions of various factors to the recent TTL variability are addressed in Sect. 3. Section 4 focuses on the importance of the vertical resolution in one climate model. A summary and discussion are presented in Sect. 5.

2 Model simulations and method description

2.1 Fully-coupled CESM-WACCM simulations

The model used here is NCAR's Community Earth System Model (CESM), version 1.0. CESM is a fully coupled model system, including an interactive ocean (POP2), land (CLM4), sea ice (CICE) and atmosphere (CAM/WACCM) component (Marsh et al., 2013). As the atmospheric component we use the Whole Atmosphere Community Climate Model (WACCM), version 4. WACCM4 is a chemistry–climate model (CCM), with detailed middle atmospheric chemistry and a finite volume dynamical core, extending from the surface to about 140 km (Marsh et al., 2013). The standard version has 66 (W_L66) vertical levels, which means about 1 km vertical resolution in the TTL and in the lower stratosphere. All simulations use a horizontal resolution of $1.9^\circ \times 2.5^\circ$ (latitude $\times$ longitude) for the atmosphere and approximately 1 degree for the ocean.

Table 1 gives an overview of all coupled CESM simulations. A control run was performed from 1955 to 2099 (Natural run hereafter), with all natural forcing including spectrally resolved solar variability (Lean et al., 2005), a fully coupled ocean, volcanic aerosols following the SPARC (Stratospheric Processes and their Role in Climate) CCMVal (Chemistry-Climate Model Validation) REF-B2 scenario recommendations (see details in SPARC-CCMVal, 2010) and a nudged QBO. The QBO is nudged by relaxing the modeled tropical zonal winds to observations between 22° S and N, using a Gaussian weighting function with a half width of 10° decaying latitudinally from the equator. Full vertical relaxation extends from 86 to 4 hPa, which is half the strength of the level below and above this range and zero for all other levels (see details in Matthes et al., 2010; Hansen et al., 2013). The QBO forcing time series in CESM is determined from the observed climatology of 1953-2004 via filtered spectral decomposition of that climatology. This gives a set of Fourier coefficients that can be expanded for any day and year in the past and the future. Anthropogenic forcings like GHGs and ozone depleting substances (ODSs) are set to constant 1960s conditions. Using the Natural run as a reference, a series of four sensitivity experiments were performed by systematically switching on or off several factors.

The SolarMean run uses constant solar cycle values averaged over the past 4 observed solar cycles; the FixedSST run uses monthly varying climatological SSTs calculated from the Natural run, and therefore neglects variability from varying SSTs such as ENSO; in the NOQBO run the QBO nudging has been switched off which means weak zonal mean easterly winds develop in the tropical stratosphere. An additional simulation RCP85, uses the same forcings as the Natural run, but in addition includes increases in anthropogenic GHGs and ODSs forcings. These forcings are based on observations from 1955 to 2005, after which they follow the Representative Concentration Pathways (RCPs) RCP8.5 scenario (Meinshausen et al., 2011).

2.2 WACCM atmospheric stand-alone simulations

Instead of using the fully coupled CESM-WACCM version, WACCM can be integrated in an atmospheric stand-alone configuration, with prescribed SSTs and sea ice. Beside the standard version with 66 vertical levels (W_L66), we have also performed simulations with a finer vertical resolution, with 103 vertical levels and about 300 m vertical resolution in the TTL and lower stratosphere (W_L103) (Gettelman and Birner, 2007; Wang et al., 2013).

With the atmospheric stand-alone version, an ensemble of three experiments was performed over the recent decade 2001–2010 with both WACCM versions (W_L66, W_L103) (see Table 2). Observed SSTs and spectrally resolved solar fluxes were used to produce the most realistic simulations of atmospheric variability over the past decade (2001–2010). The QBO is nudged using the same method as in the fully-coupled runs discussed above. GHGs and ODSs are based on observations for the first 5 years (2001–2005) and then follow the IPCC RCP4.5 scenario for the next 5 years (2005–2010), since no observational data were available when the simulations were started. Atmospheric aerosols were relatively constant between 2001 and 2010 since no strong volcanic eruptions occurred, and are the same as in the CESM-WACCM runs described above. All the forcings considered in this study are available from the CESM model input data repository (https://svn-ccsm-inputdata.cgd.ucar.edu/trunk/inputdata/). An additional run (W_Aerosol) was performed using the W_L103 version with observed, more

realistic stratospheric aerosol forcing from the Chemistry-Climate Model Initiative (CCMI, http://www.met.reading.ac.uk/ccmi/).

2.3 Estimation of factor contributions

For a pair of reference and single-factor runs (e.g. Natural and SolarMean), all configuration and drivers are the same except for the long-term variability of the respective factor (e.g. Solar). Temperature differences $T_{\text{diff}}(x,t)$ between the reference and single-factor runs (e.g. Natural - SolarMean) can be estimated by a linear regression:

$$T_{\text{est}}(x,t) = c(x)X(t), \tag{1}$$

where $T_{\text{est}}(x,t)$ is an estimate of $T_{\text{diff}}(x,t)$ at each grid point (x) and each simulation time (t). $X(t)$ is the time series of the respective factor (e.g. Solar) and $c(x)$ are the coefficients of that factor at each grid point.

Then the contributions of that factor to the recent warming in the TTL can be estimated as:

$$T_{\text{fac}}(x) = c(x)b_{\text{fac}}, \tag{2}$$

where $T_{\text{fac}}(x)$ represents the factor contribution to the recent temperature trend, $c(x)$ are the coefficients and b_{fac} is the observed linear trend of that factor during 2001-2011 (Fig. 1).

The standard error (SE) can be used to estimate the uncertainty of the regressed coefficients $c(x)$, which is defined by:

$$(\text{SE})^2 = \left[\sum_{t=1}^{n} e_t^2\right] / \left[(n_{\text{eff}} - 2)\sum_{t=1}^{n}(X_t - \bar{X})^2\right], \tag{3}$$

where n is the sample size, $e = T_{\text{diff}} - T_{\text{est}}$ are the residuals, and $\bar{X}$ is the mean value. n_{eff} is the effective number of degrees of freedom, with consideration of the effect of autocorrelation, which is determined by:

$$n_{\text{eff}} = n\frac{1 - r_{\text{a}}}{1 + r_{\text{a}}}, \tag{4}$$

where r_{a} is the lag-1 autocorrelation coefficient (Wigley, 2006).

For the estimated coefficients c, the test statistics

$$t\_test = \frac{c}{SE}, \tag{5}$$

has the Student's t-distribution with $n_{\mathrm{eff}} - 2$ degrees of freedom.

Beside the regressions described above, the Pearson's correlations (r) between temperature differences (T_{diff}) and the respective factor (X) were also estimated. The test statistics

$$t\_test = r\sqrt{\frac{n_{\mathrm{eff}} - 2}{1 - r^2}}, \tag{6}$$

has the Student's t-distribution with $n_{\mathrm{eff}} - 2$ degrees of freedom, and the effective number of degrees of freedom can be estimated by:

$$\frac{1}{n_{\mathrm{eff}}} = \frac{1}{n} + \frac{2}{n} r_{\mathrm{a1}} r_{\mathrm{a2}}, \tag{7}$$

where r_{a1}, r_{a2} are the lag-1 autocorrelation coefficients of the two time series in calculating the Pearson's correlation, respectively.

Such regressions, correlations and 11-year trend estimations were applied to all factors, i.e., Solar, SSTs, QBO, GHGs and stratospheric aerosols.

Special attention is given to the region 20° S–20° N latitude and 16–21 km height, which is mainly the observed warming area in the TTL (see below). Hereafter, we use the average trend over this area to discuss the exact contribution of every factor to the temperature trend in the TTL.

2.4 Forcings in observations and model simulations

Figure 1 shows the time series of both natural and anthropogenic forcings over past and future decades in observations (black) and model experiments (blue). Observed linear trends during 2001–2011 are highlighted with straight lines.

Observations of the solar variability show that the total solar irradiance (TSI) exhibits a clear 11 year solar cycle (SC) variation of about 1 W m^{-2} between sunspot minimum (S_{min}) and sunspot maximum (S_{max}) in the past (Gray et al., 2010). The future projection in the Natural run is a repetition of the last four observed solar cycles (Fig. 1a, blue line). With a delayed and smaller amplitude return to maximum conditions, the observed TSI significantly (over 95 %) decreased during 2001-2011 (Fig. 1a, straight black line).

Figure 1b shows the variability of tropical (20° S–20° N) SSTs for the last five decades from observations (Hadley Center Updates and supplementary information available from http://www.metoffice.gov.uk/hadobs/hadisst, black lines) and up to 2099 from the Natural coupled CESM-WACCM model experiment (blue line). Both the observed and simulated tropical SSTs show a statistically significant (over 95 %) decrease from 2001 to 2011. Note that there is a strong drop in SSTs around 1992 in the model, which does not occur in observations. This might be caused by an overestimated response to the Pinatubo eruption in the CESM-WACCM model (Marsh et al., 2013; Meehl et al., 2012).

The QBO variations are represented by a pair of orthogonal time series QBO1 and QBO2, which are constructed from the equatorial zonal winds over 70-10 hPa (Randel et al., 2009). The observed QBO2 (data from the FU Berlin: http://www.geo.fu-berlin.de/en/met/ag/strat/produkte/qbo/index.html), which is the dominate mode of QBO in the tropical lower stratosphere, shows an increase (a shift towards westerlies or stronger westerlies) during 2001-2011 (Fig. 1c, straight black line). Note that this short-term linear trend of the QBO2 is sensitive to the start and ending years. However, a further analysis for 2001-2012 ending with a relative minimum of QBO2, confirms this significant increase of QBO2 (not shown).

As shown in Fig. 1d, GHGs show a steady increase after 2001. The increasing rate of global CO_2 release from 2001 to 2011 is close to the RCP8.5 scenario, which were used in our RCP85 run.

Similar to the GHGs, observed stratospheric aerosols (aerosol optical depth (AOD)) have been steadily increasing since 2001 (Solomon et al., 2011) in the lower stratosphere (18–32 km) (Fig. 1e). This increase in stratospheric aerosol loading is at-

tributed to a number of small volcanic eruptions and anthropogenically released aerosols transported into the stratosphere during the Asian Monsoon (Bourassa et al., 2012; Neely et al., 2013). An aerosol data set has been constructed for the CCMI project (ftp://iacftp.ethz.ch/pub_read/luo/ccmi/) and is similar to the data described by Solomon et al. (2011). The comparison of the two experiments with different AOD data sets will shed light on the stratospheric aerosol contribution to the observed temperature trend.

All natural and anthropogenic forcings will be discussed with respect to their contribution to the temperature variability in TTL in the following section.

3 Quantification of observed temperature variability

3.1 Observed temperature variability in the TTL

Figure 2 shows the latitude-height section of the linear temperature trends for the period 2001–2011 estimated from GPS-RO observations (see details of the GPS-RO data in Wang et al. (2013)). A remarkable and statistically significant warming occurs around the TTL between about 20° south to north and from 16 to 21 km height. The warming in the TTL is 0.9 K decade^{-1} on average, with a maximum of about 1.8 K decade^{-1} directly at the tropical tropopause around 17 to 18 km. This figure is an extension of earlier work by Schmidt et al. (2010) and Wang et al. (2013) and shows an unexpected warming, despite the steady increase in GHGs. Therefore it is interesting to study whether this warming is simply a phenomenon of the past decade and the result of internal atmospheric variability, or whether it will persist for longer and therefore modify trace gas transport from the troposphere into the stratosphere.

Note that this decadal warming in the TTL may vary in magnitude if different end years are selected due to the relative short length of the time series. The warming is weaker if end years of 2012 or 2013 are chosen (see also Figs. S1 and S2). In the following investigations, we keep the period from 2001 through 2011 to be most consistent with our stand-alone WACCM simulations (2001–2010). We will explain the temperature variability

within a time period of about one decade. This decadal variability may change sign from decade to decade if it is mainly caused by natural/internal variability. However, it is still very important to understand the reasons and mechanisms behind these internal variability modes as it might eventually enhance our decadal to multi-decadal predictive skills.

3.2 Contribution of solar variability

Figures 3a and b show the correlation between temperature differences (Natural - SolarMean) with solar forcing (TSI) in the Natural run over the whole simulation period from 1955 through 2099, as well as the estimated temperature trends during 2001 through 2011 related to a decreasing total solar irradiance (TSI). The correlation between temperature differences and TSI is relatively weak, amounts to less than 0.1 in the TTL region and is a little higher and more significant in the lower stratosphere. With such a weak positive correlation, the decreasing solar irradiance contributed to a cooling of about $0.2\ \mathrm{K\,decade^{-1}}$ in the TTL during 2001–2011.

3.3 Contribution of tropical SSTs

Figure 4 shows the correlation between temperature differences (Natural - FixedSST) with tropical (20°S-20°N) SSTs from the Natural run over the whole simulation period from 1955 through 2099, as well as the estimated temperature trends from 2001 through 2011 due to decreasing tropical SSTs. Temperature differences are closely correlated with tropical SSTs, which show strong positive correlations (up to 0.8) below and significant negative correlations (over 0.5) above the tropopause in the tropics. The strong correlation between tropical SSTs and atmospheric temperatures indicates that tropical SSTs have important impacts on the TTL temperature. A decrease in tropical SSTs contributes therefore to a statistically significant warming of $0.3\ \mathrm{K\,decade^{-1}}$ on average ($0.6\ \mathrm{K\,decade^{-1}}$ in maximum) in the TTL during 2001–2011 (Fig. 4c).

3.4 Contribution of the QBO

As described in $section2.5$, a pair of orthogonal time series of the QBO are used in the regression between temperature differences (Natural - NOQBO) and the QBO from the Natural run. Since the QBO1 mainly affects temperature at middle and upper stratosphere, only the QBO2 correlation and impacts are shown in Figure 5. QBO2 features a strong positive correlation in the TTL region, which amounts up to 0.6. An observed increase of QBO2 during 2001–2011, which means stronger westerlies, therefore contributes to a 0.2 K decade^{-1} warming on average (0.4 K decade^{-1} in maximum) in the TTL. Another effect of the QBO is the statistically significant cooling trend seen in the tropical middle stratosphere above 23 km. This QBO effect may help to explain the observed tropical cooling (see Fig. 2). However, CESM1.0 used for these simulations, cannot generate a self-consistent QBO and hence uses wind nudging, which might cause problems when estimating QBO effects on temperature variability in the tropical lower stratosphere (Marsh et al., 2013; Morgenstern et al., 2010).

3.5 Contribution of GHGs

As expected, GHGs show strong positive correlations with temperatures in the troposphere and significant negative correlations with temperatures in the stratosphere, with a switch of sign near the tropopause (about 18 km). Increasing GHGs in the RCP85 experiment tend to cool the lower stratosphere and warm the upper troposphere, but have no evident contribution around the tropopause (with a change of correlation sign at about 18 km). This is consistence with previous studies (e.g. Kim et al., 2013), which confirmed a warming at 100 hPa (below the tropopause) and a cooling at 70 hPa (above the tropopause) due to the increase of GHGs in CMIP5 (Coupled Model Intercomparison Project Phase 5) simulations.

3.6 Contribution of stratospheric aerosols

The correlations between temperature differences (W_Aerosol - W_L103) with CCMI stratospheric aerosols, as well as the contributions of increasing stratospheric aerosols to the

recent warming in the TTL are shown in Figs. 7a and b, respectively. Weak but partly significant correlations of stratospheric aerosols to temperature in the TTL can be found in Fig. 7a, with a change of correlation sign below the tropopause (about 15 km) and up to 0.2 in the lower stratosphere. The effect of increasing stratospheric aerosols during 2001–2011 is estimated to be 0.2 K decade^{-1} warming in the TTL (Fig. 7b). Note that there may exist uncertainties for this result since we have only 10 years of simulations for the W_Aerosol run.

4 Effects of the vertical resolution

To estimate not only anthropogenic and natural contributions to the recent TTL temperature variability but also the effects of the vertical resolution in the model, Figs. 8a and b show the temperature trends in the standard W_L66 run and the differences in temperature trends between the high-resolution (W_L103) and the standard (W_L66) runs, respectively. The W_L103 run (Fig. 8b) shows a statistically significant 0.5 K decade^{-1} warming on average over the past decade around the TTL, which maximizes at 1.2 K decade^{-1}. The standard W_L66 run (Fig. 8a) does not capture the warming. The only difference between the two experiments is the vertical resolution, meaning that a higher vertical resolution captures the warming in the TTL better than the standard vertical resolution, reaching up to 0.8 K decade^{-1} (Fig. 8b). Wang et al. (2013) showed that the tropical upwelling in the lower stratosphere has weakened over the past decade in the W_L103 run, while there is no significant upwelling trend in the standard vertical resolution (W_L66) run. The decreasing tropical upwelling in the W_L103 run might be the reason for the extra warming in the TTL compared to the W_L66 run, since dynamical changes would lead to adiabatic warming. More detailed investigations will be given in the following section.

4.1 Changes in the Brewer–Dobson circulation

To investigate dynamical differences between the two experiments with standard and higher vertical resolution in more detail, the Transformed Eulerian Mean (TEM) diagnos-

tics (Andrews et al., 1987) was applied to investigate differences in the wave propagation and Brewer–Dobson circulation (BDC) in the climatological mean as well as in the decadal trend.

Figure 9 shows the annual mean climatology of the BDC (arrows for the meridional and vertical wind components), the zonal mean zonal wind (blue contour lines) and the temperature (filled colours) from the W_L103 run (Fig. 9a), as well as the differences between the W_L103 and the W_L66 runs (Fig. 9c). The BDC shows an upwelling in the tropics and a downwelling through mid to high latitudes in the annual mean. With finer vertical resolution (W_L103) the model produces a stronger upwelling in the tropics (and a consistent cooling) up to the tropopause region, with westerly wind anomalies above. This strengthened tropical upwelling cannot continue further up because of the westerly wind anomalies which block the transport into the subtropics (Simpson et al., 2009; Flannaghan and Fueglistaler, 2013). Above the tropical tropopause there is less upwelling and in particular more transport from the subtropics into the tropical TTL, leading to a stronger warming around 19 km in the W_L103 experiment. These changes in the BDC indicate a strengthening of its lower branch, and a weakening at upper levels in the lower stratosphere (Lin and Fu, 2013). This is consistent with previous work by Bunzel and Schmidt (2013), which indicates a weaker upward mass flux around 70 hPa in a model experiment with higher vertical resolution.

The annual mean trends in the W_L103 experiment indicate a further strengthening of the BDC lower branch over the past decade in this simulation (Fig. 9b) and a statistically significant weakening in the lower stratosphere resulting in significant warming of 1 to 2 $\mathrm{K\,decade^{-1}}$ in the TTL. In particular the trends in the TTL are stronger in the W_L103 compared to the W_L66 experiment (Fig. 9d).

In summary, the finer vertical resolution can enhance the upward wave propagation from the tropics. This enhanced wave propagation speeds up the lower branch of the BDC in the upper troposphere and slows down the upper branch of the BDC in the lower stratosphere. These changes in the BDC and corresponding wave-mean flow interactions (not shown) finally result in the statistically significant warming in the TTL.

Bunzel and Schmidt (2013) attributed the differences in the BDC to different vertical resolutions which tend to reduce the numerical diffusion through the tropopause and the secondary meridional circulation. Our results show that the strong warming and subsequent enhanced static stability (not shown) above the tropopause may also influence wave dissipation and propagation around the tropopause. Oberländer et al. (2013) point out that an increase of tropical SSTs enhances the BDC. This is consistent with our results, which show a weakening of the BDC in the lower stratosphere following a decrease in tropical SSTs. At the same time, this response of the stratosphere to the surface can be better represented by a model with finer vertical resolution.

5 Summary and discussion

Based on a series of sensitivity simulations with NCAR's CESM-WACCM model, the relationships between different natural (solar, QBO, tropical SSTs) and anthropogenic (GHGs, ODS) factors and temperatures around TTL, as well as their contributions to the observed warming of the TTL over the past decade from 2001 through 2011 has been studied. By regressing the temperature differences between model experiments to the respective factors for the whole simulation periods between 1955 through 2099, and projecting the regressed coefficients onto the observed trends of the respective factor during 2001-2011, the contribution of each factor has been quantified in order to explain the causes of the observed recent decadal variability seen in GPS-RO data.

The SSTs show strong significant negative correlation (-0.5) with temperatures in the TTL, while the QBO2 shows a reversed pattern (0.6). The TSI and stratospheric aerosols result in weak positive correlations (0.1-0.2) with TTL temperatures. GHGs show positive correlations with temperatures in the troposphere and negative correlations with temperatures in the stratosphere, while there is no significant correlation around the tropopause.

A decrease in tropical SSTs, an increase in stratospheric aerosol loading and stronger QBO westerlies contribute each about 0.3, 0.2 and 0.2 K decade^{-1} to this warming, respectively, resulting in a total 0.7 K decade^{-1} warming, while the delay and smaller amplitude of

the current solar maximum contributes about 0.2 K decade^{-1} to a cooling. Adding all natural and anthropogenic factors, we estimate a total modeled warming of 0.5 K decade^{-1} around the TTL (Table 3), which is less than the observed 0.9 K decade^{-1} warming from GPS-RO data. One possible reason of this weak estimate is the relative low vertical resolution of the model, which strongly influences the TTL response to the surface mainly via dynamical changes, i.e. an enhancement of the lower branch of the BDC and a decrease of the upper branch in the lower stratosphere in response to decreasing tropical SSTs. This leads to a 0.8 K decade^{-1} extra warming in the TTL in the finer vertical resolution experiment as compared to the standard vertical resolution. However, in reality non-linear interactions between the different factors occur which we did not take into account in our first order linear approach. The comprehensive impact of all factors on the recent TTL warming can be estimated by the W_Aerosol run. The W_Aerosol run, with almost all observed forcings considered in this study, can be seen as the most realistic simulation. The TTL warming in the W_Aerosol run is 0.9 K decade^{-1} on average and 1.6 K decade^{-1} in maximum (Fig. 7b), which are very close to the observed trend.

According to our experiments, one of the primary factors contributing to the recent warming in the TTL is the natural variability in tropical SSTs. However, the mechanism of the TTL response to SSTs awaits further investigation. One key issue is how much improvement we can expect from using a fully-coupled ocean-atmosphere model instead of atmosphere only model with prescribed SSTs. Our W_L66 and W_L103 simulations indicate that the atmosphere-only model may not correctly reproduce the response of TTL variability to SST, but can be improved with finer vertical resolution.

Another important factor in contributing to the recent warming in the TTL is the QBO. The QBO is closely related to the tropical upwelling Flury et al. (2013). A regression of temperature differences onto the differences in the vertical component of BDC between the Natural and NOQBO run, shows a very similar result than the regression of temperature differences onto the QBO time series (not shown). The QBO may influence the TTL temperature by modifying the BDC.

Fig. S3 clearly shows decadal to multidecadal fluctuations in TTL temperatures from both, the Modern Era Retrospective-analysis for Research and Applications (MERRA) reanalysis data, and our Natural and RCP85 runs, which provide strong support to the internal variability dominated TTL warming over the past decade.

The external forcings (solar, GHGs, ODS) contribute relatively little to the temperature variability in the TTL, except for the stratospheric aerosols. Internal variability, i.e. the QBO and tropical SSTs, seem to be mainly responsible for the recent TTL warming.

Acknowledgements. W. Wang is supported by a fellowship of the China Scholarship Council (CSC) at FU Berlin. This work was also performed within the Helmholtz-University Young Investigators Group NATHAN, funded by the Helmholtz-Association through the president's Initiative and Networking Fund, and the GEOMAR – Helmholtz-Zentrum für Ozeanforschung in Kiel. The model calculations have been performed at the Deutsche Klimarechenzentrum (DKRZ) in Hamburg, Germany. We thank F. Hansen, C. Petrick, R. Thiéblemont and S. Wahl for carrying out some of the simulations. We appreciate discussion about the statistical methods with D. Maraun and the help with grammar checking of L. Neef .

The service charges for this open access publication have been covered by a Research Centre of the Helmholtz Association.

References

Andrews, D. G.: An Introduction to Atmospheric Physics, Cambridge University Press, New York, 2010.

Andrews, D. G., Holton, J. R., and Leovy, C. B.: Middle Atmosphere Dynamics, vol. 40, Academic Press, San Diego, 1987.

Baldwin, M. P., Gray, L. J., Dunkerton, T. J., Hamilton, K., Haynes, P. H., Randel, W. J., Holton, J. R., Alexander, M. J., Hirota, I., Horinouchi, T., Jones, D. B. A., Kinnersley, J. S., Marquardt, C., Sato, K., and Takahashi, M.: The quasi-biennial oscillation, Rev. Geophys., 39, 179–229, doi:10.1029/1999RG000073, 2001.

Balmaseda, M. A., Trenberth, K. E., and Källén, E.: Distinctive climate signals in reanalysis of global ocean heat content, Geophys. Res. Lett., 40, 1754–1759, doi:10.1002/grl.50382, 2013.

Bourassa, A. E., Robock, A., Randel, W. J., Deshler, T., Rieger, L. A., Lloyd, N. D., Llewellyn, E. T., and Degenstein, D. A.: Large volcanic aerosol load in the stratosphere linked to Asian monsoon transport, Science, 337, 78–81, doi:10.1126/science.1219371, 2012.

Bunzel, F. and Schmidt, H.: The Brewer–Dobson circulation in a changing climate: impact of the model configuration, J. Atmos. Sci., 70, 1437–1455, doi:10.1175/JAS-D-12-0215.1, 2013.

Butchart, N.: The Brewer–Dobson circulation, Rev. Geophys., 52, 157–184, doi:10.1002/2013RG000448, 2014.

Butchart, N., Cionni, I., Eyring, V., Shepherd, T. G., Waugh, D. W., Akiyoshi, H., Austin, J., Bruhl, C., Chipperfield, M. P., Cordero, E., Dameris, M., Deckert, R., Dhomse, S., Frith, S. M., Garcia, R. R., Gettelman, A., Giorgetta, M. A., Kinnison, D. E., Li, F., Mancini, E., McLandress, C., Pawson, S., Pitari, G., Plummer, D. A., Rozanov, E., Sassi, F., Scinocca, J. F., Shibata, K., and Tian, W.: Chemistry-climate model simulations of twenty-first century stratospheric climate and circulation changes, J. Climate, 23, 5349–5374, doi:10.1175/2010JCLI3404.1, 2010.

Dessler, A. E., Schoeberl, M. R., Wang, T., Davis, S. M., and Rosenlof, K. H.: Stratospheric water vapor feedback., P. Natl. Acad. Sci. USA, 110, 18087–18091, doi:10.1073/pnas.1310344110, 2013.

Dessler, A., Schoeberl, M., Wang, T., Davis, S., Rosenlof, K., and Vernier, J.-P.: Variations of stratospheric water vapor over the past three decades, J. Geophys. Res., 119, 12–588, doi:10.1002/2014JD021712, 2014.

Engel, A., Mobius, T., Bonisch, H., Schmidt, U., Heinz, R., Levin, I., Atlas, E., Aoki, S., Nakazawa, T., Sugawara, S., Moore, F., Hurst, D., Elkins, J., Schauffler, S., Andrews, A., and Boering, K.: Age of stratospheric air unchanged within uncertainties over the past 30 years, Nat. Geosci., 2, 28–31, doi:10.1038/ngeo388, 2009.

England, M. H., McGregor, S., Spence, P., Meehl, G. A., Timmermann, A., Cai, W., Gupta, A. S., McPhaden, M. J., Purich, A., and Santoso, A.: Recent intensification of wind-driven circulation in the Pacific and the ongoing warming hiatus, Nature Climate Change, 4, 222–227, doi:10.1038/nclimate2106, 2014.

Flannaghan, T. and Fueglistaler, S.: The importance of the tropical tropopause layer for equatorial Kelvin wave propagation, J. Geophys. Res., 118, 5160–5175, doi:10.1002/jgrd.50418, 2013.

Flury, T., Wu, D. L., and Read, W. G.: Variability in the speed of the Brewer–Dobson circulation as observed by Aura/MLS, Atmos. Chem. Phys., 13, 4563–4575, doi:10.5194/acp-13-4563-2013, 2013.

Fueglistaler, S., Dessler, A., Dunkerton, T., Folkins, I., Fu, Q., and Mote, P. W.: Tropical tropopause layer, Rev. Geophys., 47, 1004, doi:10.1029/2008RG000267, 2009.

Fueglistaler, S., Liu, Y., Flannaghan, T., Haynes, P., Dee, D., Read, W., Remsberg, E., Thomason, L., Hurst, D., Lanzante, J., et al.: The relation between atmospheric humidity and temperature trends for stratospheric water, J. Geophys. Res., 118, 1052–1074, doi:10.1002/jgrd.50157, 2013.

Fyfe, J. C. and Gillett, N. P.: Recent observed and simulated warming, Nature Clim. Change, 4, 150–151, doi:10.1038/nclimate2111, 2014.

Fyfe, J. C., Gillett, N. P., and Zwiers, F. W.: Overestimated global warming over the past 20 years, Nature Climate Change, 3, 767–769, doi:10.1038/nclimate1972, 2013.

Gettelman, A. and Birner, T.: Insights into tropical tropopause layer processes using global models, J. Geophys. Res., 112, D23104, doi:10.1029/2007JD008945, 2007.

Gettelman, A. and Forster, P. D. F.: A climatology of the tropical tropopause layer, J. Meteor. Soc. Jpn., 80, 911–924, doi:10.2151/jmsj.80.911, 2002.

Gettelman, A., Birner, T., Eyring, V., Akiyoshi, H., Bekki, S., Brühl, C., Dameris, M., Kinnison, D. E., Lefevre, F., Lott, F., Mancini, E., Pitari, G., Plummer, D. A., Rozanov, E., Shibata, K., Stenke, A., Struthers, H., and Tian, W.: The Tropical Tropopause Layer 1960–2100, Atmos. Chem. Phys., 9, 1621–1637, doi:10.5194/acp-9-1621-2009, 2009.

Gray, L. J., Beer, J., Geller, M., Haigh, J. D., Lockwood, M., Matthes, K., Cubasch, U., Fleitmann, D., Harrison, G., Hood, L., Luterbacher, J., Meehl, G. A., Shindell, D., van Geel, B., and White, W.: Solar influences on climate, Rev. Geophys., 48, RG4001, doi:10.1029/2009RG000282, 2010.

Grise, K. M. and Thompson, D. W.: Equatorial planetary waves and their signature in atmospheric variability, J. Atmos. Sci., 69, 857–874, doi:10.1175/JAS-D-11-0123.1, 2012.

Grise, K. M. and Thompson, D. W.: On the signatures of equatorial and extratropical wave forcing in tropical tropopause layer temperatures, J. Atmos. Sci., 70, 1084–1102, doi:10.1175/JAS-D-12-0163.1, 2013.

Hansen, F., Matthes, K., and Gray, L.: Sensitivity of stratospheric dynamics and chemistry to QBO nudging width in the chemistry–climate model WACCM, J. Geophys. Res., 118, 10–464, doi:10.1002/jgrd.50812, 2013.

Kawatani, Y. and Hamilton, K.: Weakened stratospheric quasibiennial oscillation driven by increased tropical mean upwelling, Nature, 497, 478–481, doi:10.1038/nature12140, 2013.

Kim, J., Grise, K. M., and Son, S.: Thermal characteristics of the cold-point tropopause region in CMIP5 models, J. Geophys. Res., 118, 8827–8841, doi:10.1002/jgrd.50649, 2013.

Kosaka, Y. and Xie, S.-P.: Recent global-warming hiatus tied to equatorial Pacific surface cooling, Nature, 501, 403–407, doi:10.1038/nature12534, 2013.

Lean, J., Rottman, G., Harder, J., and Kopp, G.: SORCE contributions to new understanding of global change and solar variability, Sol. Phys., 230, 27–53, doi:10.1007/s11207-005-1527-2, 2005.

Li, F., Austin, J., and Wilson, J.: The strength of the Brewer–Dobson circulation in a changing climate: coupled chemistry-climate model simulations, J. Climate, 21, 40–57, doi:10.1175/2007JCLI1663.1, 2008.

Lin, P. and Fu, Q.: Changes in various branches of the Brewer–Dobson circulation from an ensemble of chemistry climate models, J. Geophys. Res., 118, 73–84, doi:10.1029/2012JD018813, 2013.

Marsh, D. R., Mills, M. J., Kinnison, D. E., Lamarque, J.-F., Calvo, N., and Polvani, L. M.: Climate change from 1850 to 2005 simulated in CESM1 (WACCM), J. Climate, 26, 7372–7391, doi:10.1175/JCLI-D-12-00558.1, 2013.

Matthes, K., Marsh, D. R., Garcia, R. R., Kinnison, D. E., Sassi, F., and Walters, S.: Role of the QBO in modulating the influence of the 11 year solar cycle on the atmosphere using constant forcings, J. Geophys. Res., 115, 18110, doi:10.1029/2009JD013020, 2010.

Meehl, G. A., Washington, W. M., Arblaster, J. M., Hu, A., Teng, H., Tebaldi, C., Sanderson, B. N., Lamarque, J.-F., Conley, A., Strand, W. G., and White, J. B.: Climate system response

to external forcings and climate change projections in CCSM4, J. Climate, 25, 3661–3683, doi:10.1175/JCLI-D-11-00240.1, 2012.

Meinshausen, M., Smith, S. J., Calvin, K., Daniel, J. S., Kainuma, M. L. T., Lamarque, J.-F., Matsumoto, K., Montzka, S., Raper, S., Riahi, K., Thomson, A., Velders, G. J. M., and van Vuuren, D. P.: The RCP greenhouse gas concentrations and their extensions from 1765 to 2300, Climatic Change, 109, 213–241, doi:10.1007/s10584-011-0156-z, 2011.

Morgenstern, O., Giorgetta, M. A., Shibata, K., Eyring, V., Waugh, D. W., Shepherd, T. G., Akiyoshi, H., Austin, J., Baumgaertner, A. J. G., Bekki, S., Braesicke, P., Brühl, C., Chipperfield, M. P., Cugnet, D., Dameris, M., Dhomse, S., Frith, S. M., Garny, H., Gettelman, A., Hardiman, S. C., Hegglin, M. I., Jöckel, P., Kinnison, D. E., Lamarque, J.-F., Mancini, E., Manzini, E., Marchand, M., Michou, M., Nakamura, T., Nielsen, J. E., Olivié, D., Pitari, G., Plummer, D. A., Rozanov, E., Scinocca, J. F., Smale, D., Teyssèdre, H., Toohey, M., Tian, W., and Yamashita, Y.: Review of the formulation of present-generation stratospheric chemistry-climate models and associated external forcings, J. Geophys. Res., 115, D00M02, doi:10.1029/2009JD013728, 2010.

Neely, R. R., Toon, O. B., Solomon, S., Vernier, J. P., Alvarez, C., English, J. M., Rosenlof, K. H., Mills, M. J., Bardeen, C. G., Daniel, J. S., and Thayer, J. P.: Recent anthropogenic increases in SO_2 from Asia have minimal impact on stratospheric aerosol, Geophys. Res. Lett., 40, 999–1004, doi:10.1002/grl.50263, 2013.

Oberländer, S., Langematz, U., and Meul, S.: Unraveling impact factors for future changes in the Brewer–Dobson circulation, J. Geophys. Res., 118, 10–296, doi:10.1002/jgrd.50775, 2013.

Randel, W. J. and Jensen, E. J.: Physical processes in the tropical tropopause layer and their roles in a changing climate, Nat. Geosci., 6, 169–176, doi:10.1038/ngeo1733, 2013.

Randel, W. J., Shine, K. P., Austin, J., Barnett, J., Claud, C., Gillett, N. P., Keckhut, P., Langematz, U., Lin, R., Long, C., Mears, C., Miller, A., Nash, J., Seidel, D. J., Thompson, D. W. J., Wu, F., and Yoden, S.: An update of observed stratospheric temperature trends, J. Geophys. Res., 114, D02107, doi:10.1029/2008JD010421, 2009.

Richter, J. H., Solomon, A., and Bacmeister, J. T.: On the simulation of the quasi-biennial oscillation in the Community Atmosphere Model, version 5, Journal of Geophysical Research: Atmospheres, 119, doi:10.1002/2013JD021122, 2014.

Schmidt, T., Wickert, J., and Haser, A.: Variability of the upper troposphere and lower stratosphere observed with GPS radio occultation bending angles and temperatures, Adv. Space. Res., 46, 150–161, doi:10.1016/j.asr.2010.01.021, 2010.

Shepherd, T. G. and McLandress, C.: A robust mechanism for strengthening of the Brewer–Dobson circulation in response to climate change: critical-layer control of subtropical wave breaking, J. Atmos. Sci., 68, 784–797, doi:10.1175/2010JAS3608.1, 2011.

Simpson, I. R., Blackburn, M., and Haigh, J. D.: The role of eddies in driving the tropospheric response to stratospheric heating perturbations, J. Atmos. Sci., 66, 1347–1365, doi:10.1175/2008JAS2758.1, 2009.

Solomon, S., Rosenlof, K. H., Portmann, R. W., Daniel, J. S., Davis, S. M., Sanford, T. J., and Plattner, G.-K.: Contributions of stratospheric water vapor to decadal changes in the rate of global warming, Science, 327, 1219–1223, doi:10.1126/science.1182488, 2010.

Solomon, S., Daniel, J., Neely, R., Vernier, J.-P., Dutton, E., and Thomason, L.: The persistently variable "background" stratospheric aerosol layer and global climate change, Science, 333, 866–870, doi:10.1126/science.1206027, 2011.

SPARC-CCMVal: SPARC Report on the Evaluation of Chemistry-Climate Models, SPARC Report 5, WCRP-132, WMO/TD-1526, 2010.

Stiller, G. P., von Clarmann, T., Haenel, F., Funke, B., Glatthor, N., Grabowski, U., Kellmann, S., Kiefer, M., Linden, A., Lossow, S., and López-Puertas, M.: Observed temporal evolution of global mean age of stratospheric air for the 2002 to 2010 period, Atmos. Chem. Phys., 12, 3311–3331, doi:10.5194/acp-12-3311-2012, 2012.

Wang, J. S., Seidel, D. J., and Free, M.: How well do we know recent climate trends at the tropical tropopause?, J. Geophys. Res., 117, 09 118, doi:10.1029/2012JD017444, 2012.

Wang, W., Matthes, K., Schmidt, T., and Neef, L.: Recent variability of the tropical tropopause inversion layer, Geophys. Res. Lett., 40, 6308–6313, doi:10.1002/2013GL058350, 2013.

Wigley, T.: Appendix A: Statistical issues regarding trends, in: Temperature Trends in the Lower Atmosphere: Steps for Understanding and Reconciling Differences, edited by: Karl, T. R., Hassol, S. J., Miller, C. D., and Murray, W. L., A Report by Climate Change Science Program and the Subcommittee on Global Change Research, Washington, DC, USA, UNT Digital Library, 129–139, 2006.

Zhou, X.-L., Geller, M. A., and Zhang, M.: Cooling trend of the tropical cold point tropopause temperatures and its implications, J. Geophys. Res., 106, 1511–1522, doi:10.1029/2000JD900472, 2001.

Table 1. Overview of fully-coupled CESM-WACCM simulations (1955–2099).

Simulations	Natural Forcings	GHGs
Natural	All natural forcings, including transit solar variability, fully coupled ocean, prescribed volcanic aerosols and nudged QBO	Fixed GHGs to 1960s state
SolarMean	As Natural run, but with fixed solar radiation	Fixed
FixedSST	As Natural run, but with fixed SSTs	Fixed
NOQBO	As Natural run, but without QBO nudging	Fixed
RCP85	As Natural run	RCP8.5 scenario

Table 2. Overview of WACCM atmospheric stand-alone simulations (2001–2010).

Simulations	Number of Simulations	Vertical levels	Forcings	Stratospheric aerosols
W_L103	3	103	Observed solar variability and SSTs, nudged QBO, GHGs in RCP4.5 scenario	Volcanic aerosols from CCMVal-2
W_L66	3	66	As W_L103	As W_L103
W_Aerosol	1	103	As W_L103	Stratospheric aerosols from CCMI

Table 3. Summary of contributions from the varying factors to the observed TTL warming between 2001 and 2011, in the region 20° S–20° N latitude and 16–20 km

Factors	Solar	SSTs	QBO	GHGs	Aerosols	**Total**
Contribution (K decade^{-1})	-0.2	0.3	0.2	0.0	0.2	**0.5**
Observation						**0.9**
Vertical Resolution						0.8

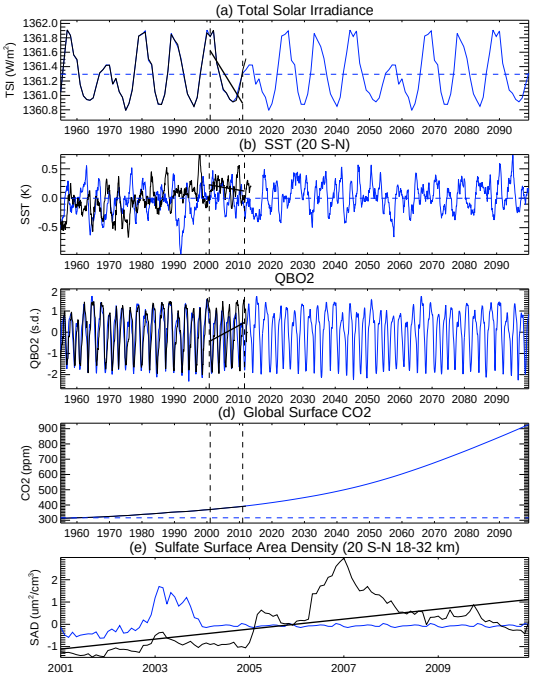

Figure 1. Time series of forcing data sets used for the simulations from 1955 through 2099. **(a)** TSI from observations (black), *Natural* (solid blue) and *SolarMean* (dashed blue) runs. **(b)** SST anomalies from HadISSTs (black), *Natural* (solid blue) and *FixedSST* (dashed blue) runs. **(c)** QBO2 (see text for details) from observations (black) and *Natural* (solid blue) run. **(d)** Global surface CO_2 concentration from observations (black, overlapped with the blue line), *RCP85* (solid blue) and *Natural* (dashed blue) runs. **(e)** AOD (532 nm, 18–32 km) from the CCMI (black) and the CCMVal2 (blue) projects for the time 2001–2010. The black solid straight lines in each subfigure are the linear fits of the respective forcing during 2001-2011.

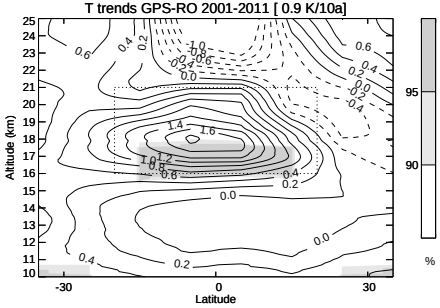

Figure 2. Latitude-height section of linear temperature trends over the past decade (2001–2011) from *GPS-RO* data over a height range from 10 to 25 km and 35° S to 35° N latitude; contour interval: 0.2 K decade^{-1}. Grey shading represents the statistical significance for the trends.

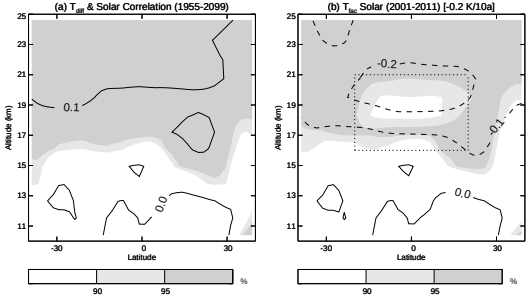

Figure 3. (a) Latitude-height sections of correlations between temperature differences (*Natural* - *SolarMean*) and solar TSI in the *Natural* run over the whole period (1955-2099); contour interval: 0.1; Grey shading represents statistically significant correlations, with Students' T test. **(b)** The regressed contributions of solar TSI to the TTL temperature trends during 2001-2011 (Eq. 2); contour interval: 0.1 K decade^{-1}; Grey shading represents statistically significant regressions. See text for details on the calculation of the regressed trend, and the testing of the statistical significance. The decadal temperature trend in the title is the mean value from the dashed box.

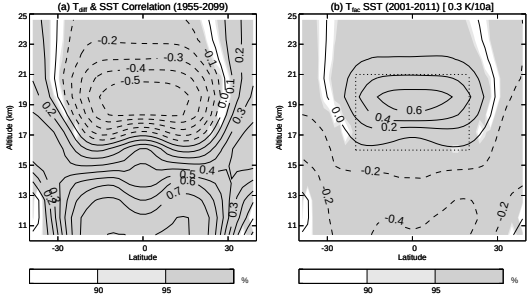

Figure 4. Same as Fig. 3, but for the impact of tropical SSTs by comparing the *Natural* and *FixedSST* runs. contour interval: **(a)** 0.1 and **(b)** 0.2 K decade^{-1}.

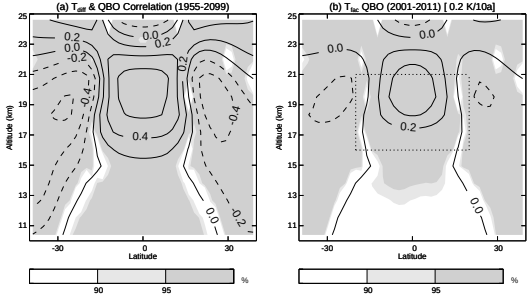

Figure 5. Same as Fig. 3, but for the impact of the QBO2 (see text for details) by comparing the *Natural* and the *NOQBO* experiments; contour interval: **(a)** 0.2 and **(b)** 0.2 K decade^{-1}.

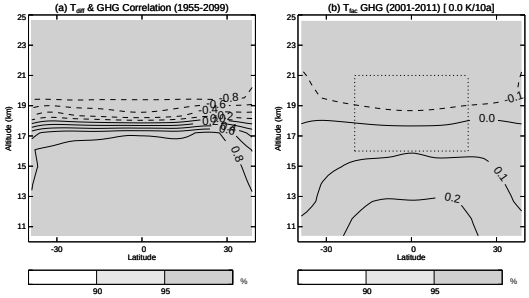

Figure 6. Same as Fig. 3, but for the impact of anthropogenic forcings (GHGs) by comparing the *Natural* and *RCP85* experiments; contour interval: **(a)** 0.2 and **(b)** 0.1 K decade^{-1}.

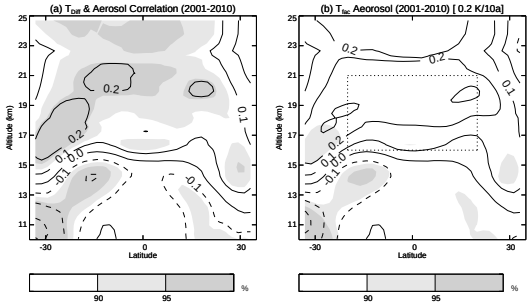

Figure 7. Same as Fig. 3, but for the impact of stratospheric aerosols by comparing the *W_L103* and the *W_Aerosol* experiments. contour interval: **(a)** 0.1 and **(b)** 0.1 K decade^{-1}. The temperatures in the *W_L103* run were calculated from a three member ensemble mean.

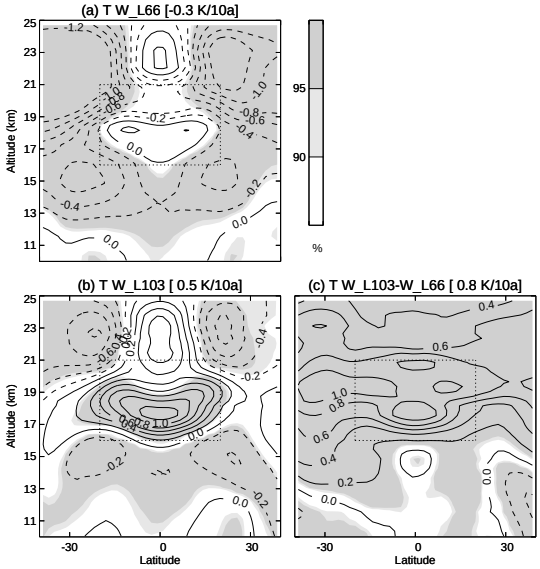

Figure 8. (a, b) Latitude-height sections of temperature trends over 2001-2010 from the *W_L103* and *W_L66* experiments, respectively. **(c)** The differences between **(a)** and **(b)**. contour interval: 0.2 K decade^{-1} and grey shading represents statistically significant trends. The temperature trends in the *W_L103* and *W_L66* runs are calculated by multiple linear regression for each three simulations.

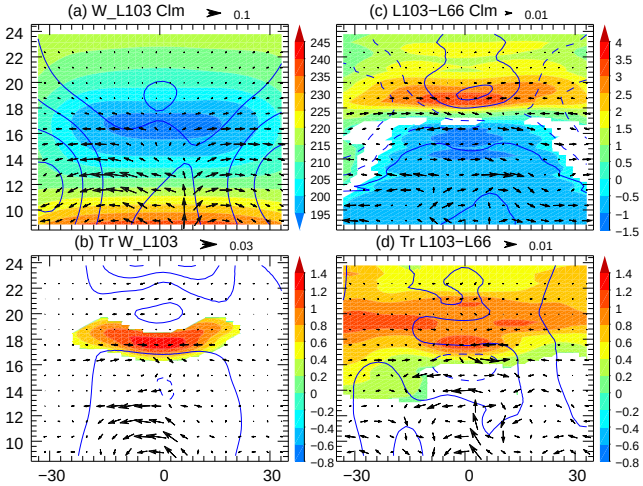

Figure 9. (a) Annual mean climatological zonal mean zonal wind (contours, contour interval 10 m s^{-1}, dashed lines indicate easterly winds), BDC vector (arrows, scaled with the square root of pressure) and temperature (colour shadings) for the *W_L103* experiment from 8 to 25 km and 35° S through 35° N. **(c)** Differences of the zonal mean zonal wind (contour interval 1.0 m s^{-1}), BDC vector and temperature (colour shadings indicate 95 % statistical significances) between the *W_L103* and the *W_L66* experiments. (**b** and **d**) Same as **(a)** and **(c)**, but for the linear trends from 2001 to 2010. The shadings in **(b)** and **(d)** indicate 95 % statistical significance. The contour intervals are 2 m s^{-1} and 1 m s^{-1} in **(c)** and **(d)**, respectively.